Material Solubility-Photovoltaic Performance Relationship in the Design of Novel Fullerene Derivatives for Bulk Heterojunction Solar Cells

By *Pavel A. Troshin,* Harald Hoppe, Joachim Renz, Martin Egginger, Julia Yu. Mayorova, Andrey E. Goryachev, Alexander S. Peregudov, Rimma N. Lyubovskaya, Gerhard Gobsch, N. Serdar Sariciftci,* and Vladimir F. Razumov*

The preparation of 27 different derivatives of C_{60} and C_{70} fullerenes possessing various aryl (heteroaryl) and/or alkyl groups that are appended to the fullerene cage via a cyclopropane moiety and their use in bulk heterojunction polymer solar cells is reported. It is shown that even slight variations in the molecular structure of a compound can cause a significant change in its physical properties, in particular its solubility in organic solvents. Furthermore, the solubility of a fullerene derivative strongly affects the morphology of its composite with poly(3-hexylthiophene), which is commonly used as active material in bulk heterojunction organic solar cells. As a consequence, the solar cell parameters strongly depend on the structure and the properties of the fullerene-based material. The power conversion efficiencies for solar cells comprising these fullerene derivatives range from negligibly low (0.02%) to considerably high (4.1%) values. The analysis of extensive sets of experimental data reveals a general dependence of all solar cell parameters on the solubility of the fullerene derivative used as acceptor component in the photoactive layer of an organic solar cell. It is concluded that the best material combinations are those where donor and acceptor components are of similar and sufficiently high solubility in the solvent used for the deposition of the active layer.

1. Introduction

During the past decade organic photovoltaics has been the subject of intensive research worldwide.[1–5] As a result, the power conversion efficiencies of fullerene-polymer solar cells were boosted from only 0.04% in 1993[6] to the commercially interesting level of 5–6% in 2006–2007.[7–9] The evolution of organic solar cells is described in detail in recent review papers.[1,4,5] An important breakthrough was achieved when pristine fullerene C_{60} was replaced by its highly soluble derivative PCBM (phenyl-C_{61}-butyric acid methyl ester).[10] The optimization of the active layer morphology in MDMO-PPV-[60]PCBM solar cells resulted in power conversion efficiencies approaching 2.5–2.7%,[11,12] with a further slight improvement to up to 3.0% being achieved by combining MDMO-PPV with a derivative of [70]fullerene called [70]PCBM which has a broader absorption in the visible region than [60]PCBM.[13]

The next step in the development of organic photovoltaics was the application of regioregular head-to-tail P3HT as a donor material.[14] Thermally annealed blends of P3HT and [60]PCBM yielded solar cells with $\eta \sim 4\%$ as reproduced by many groups worldwide.[15–18] Some researchers report even higher efficiencies of 4.9–5.5% for this system.[19]

At present there is a race to develop novel donor polymers that further improve organic solar cells by increasing the open circuit voltage (V_{OC}) or raising the short circuit current (I_{SC}). A few known poly(fluorene) copolymers exhibit V_{OC}- and η-values of $\sim 1000\,mV$ and 2–4%, respectively, in solar cells with PCBM as acceptor.[20–22] Very recently an example of a low band-gap copolymer comprising cyclopentadithiophene and benzothiadiazole units was successfully used to achieve power conversion efficiencies ranging between 3.2–5.5% in single layer devices and 6.5% in tandem cells.[7,8,23]

[*] Dr. P. A. Troshin, J. Yu. Mayorova, A. E. Goryachev, Prof. R. N. Lyubovskaya, Prof. V. F. Razumov
Institute of Problems of Chemical Physics of the Russian Academy of Sciences
Semenov Prospect 1, Chernogolovka, Moscow Region
142432 (Russia)
E-mail: troshin@cat.icp.ac.ru

Dr. H. Hoppe, J. Renz, Prof. G. Gobsch
Technical University Ilmenau, Institute of Physics
Weimarer Str. 32
Ilmenau, 98693 (Germany)

M. Egginger, Prof. N. Serdar. Sariciftci
Linz Institute for Organic Solar Cells (LIOS), Johannes Kepler University Linz Altenbergerstrasse 69, Linz, A-4040 (Austria)

Prof. A. S. Peregudov
A. N. Nesmeyanov Institute of Organoelement Compounds 1 Vavylova St. 28, B-334, Moscow, 119991 (Russia)

WILEY
InterScience®
DISCOVER SOMETHING GREAT

Surprisingly, PCBM is still considered the most advanced acceptor material for organic solar cells,[4] although one may question if PCBM is compatible with the huge diversity of novel polymers. The frequently observed poor device performance when testing new donor polymers with PCBM might be partially related to an incompatibility between the tested new polymer and PCBM. There is a considerable need for a fundamental understanding of the interactions between the fullerene derivatives on the one side and the polymers that determine the blend morphology on the other.[5] To date, there are no detailed explanations in the literature of how the molecular structures and properties of materials correlate with their performance in solar cells.

In this work we designed a large family of novel fullerene derivatives and investigated them as materials in polymer bulk heterojunction solar cells. Analysis of the obtained data was expected to provide insight into how the modification of the structure (and thereby the properties) of a fullerene derivative can affect the solar cell performance and/or the morphology of its blend with P3HT.

2. Results and Discussion

2.1. Molecular Structures of the Fullerene Compounds

The molecular structures of prepared fullerene derivatives are shown in Figure 1. Most of them are cyclopropane derivatives of fullerenes called methanofullerenes which closely resemble the structure of well-known [60]PCBM (1), which is a widely utilized material for solution processed organic solar cells. The synthesis of PCBM was first carried out by Hummelen, Wudl, and co-workers who developed a special procedure for the cyclopropanation of fullerenes based on the in situ formation of a reactive diazocompound from tosylhydrazone and sodium methoxide.[24]

PCBM was considered as the starting point for the design of our compounds. There are two substituents in the cyclopropane ring of PCBM that can be altered: i) the phenyl ring (the aromatic part) and ii) the 3-(methoxycarbonyl)propyl group (the aliphatic part). As for modifying the aromatic part the phenyl ring was replaced with a 4-methoxyphenyl (12), a 2-thienyl (3, 17–21, 24), and a 2-furyl (4) group. Some synthesized compounds (25–27) have no aromatic group at all, but possess two solubilizing, aliphatic moieties of the same (25) or different size (26–27) instead. Aliphatic tails of the fullerene derivatives were altered with the intention of attaining a reasonable solubility in organic solvents and to provide some compatibility with the n-hexyl side chains of the donor polymer P3HT. Approximately half of the prepared materials comprise propionic acid ester (–CH$_2$CH$_2$COOR) residues in their molecular framework (6–21, 25). Some compounds just have an aromatic ring and a normal alkyl chain appended to the cyclopropane ring that is linked to the fullerene cage (22–24). The structure of compound 24 is quite intriguing since it possesses only thienyl and n-hexyl substituents, hence closely resembles the repetitive unit of P3HT.

Synthesis of the methanofullerenes was carried out according to one of the three conventional synthetic routes illustrated in Scheme 1. The majority of compounds was synthesized according to the tosylhydrazone route I developed by Hummelen, Wudl, and co-workers,[24] compound 26 was obtained via the malonic acid ester route II introduced by Bingel, Hirsch and co-workers,[25,26] and 27 was prepared via a sulfonium ylide route III suggested by Wilson and co-workers.[27]

All fullerene derivatives were characterized by ^{1}H and ^{13}C NMR spectroscopy. 2D H-H COSY and H-C HSQC experiments were carried out for some representative compounds in order to verify their structures and to confirm the assignment of the one-dimensional ^{1}H and ^{13}C NMR data. These data will be published elsewhere.
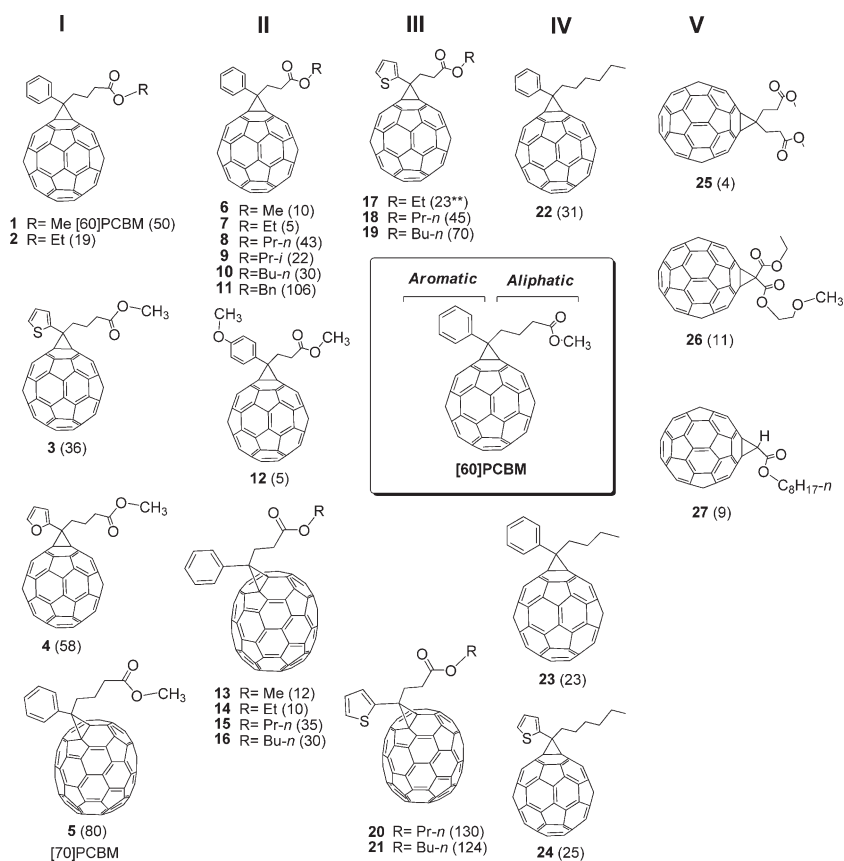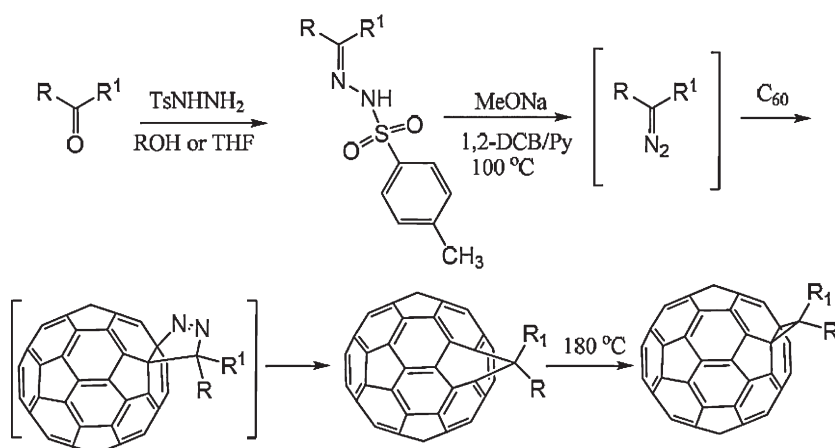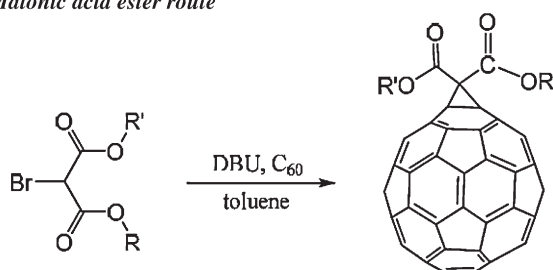

Figure 1. Molecular structures of the synthesized and investigated fullerene derivatives. Column I: aryl (hetero-aryl)-C$_{61(71)}$-butyric acid esters; column II: aryl-C$_{61(71)}$-propionic acid esters; column III: 2-thienyl- C$_{61(71)}$-propionic acid esters; column IV: fullerene derivatives without carboxyl groups; column V: fullerene derivatives without aromatic substituent. The solubility of individual compounds in chlorobenzene is given in brackets (in mg · mL^{-1}). The value marked with ** corresponds to the solubility of compound **17** in carbon disulphide (the solubility in chlorobenzene was lower than 1 mg · mL^{-1}).
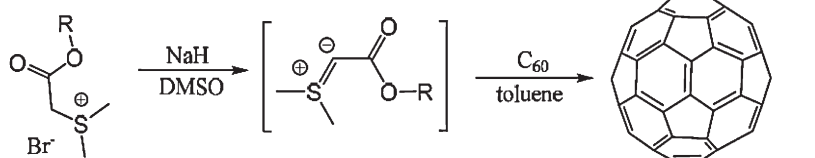
I. Tosylhydrazone route

II. Malonic acid ester route

III. Sulfonium ylide route

Scheme 1. Synthesis routes of fullerene derivatives.

2.2. Cyclic Voltammetry Study of the Fullerene Derivatives

The prepared methanofullerenes have quite similar molecular structures: one cyclopropane ring with two substituents is attached to a fullerene cage. Such similarity in molecular structures of the compounds gives rise to the expectation that the electronic properties of these compounds, in particular frontier orbital energy levels, should also be very similar. Indeed, the first reduction potential (i.e., the potential at which mono-anions are formed from neutral molecules) measured for a broad variety of investigated fullerene derivatives is virtually equal to that of PCBM (Table 1).[28] This leads to the conclusion that all studied fullerene compounds have a similar energy level for the lowest unoccupied molecular orbital (LUMO) which is filled upon electrochemical reduction of neutral species to mono-anions. It is well known that the difference between the LUMO energy of a given fullerene derivative and the HOMO (highest occupied molecular orbital) energy of a donor polymer determines the maximal open circuit voltage V_{OC} attainable in bulk heterojunc-

tion solar cells.[29,30] Therefore, taking only the energy levels of the materials into account, one would expect similar V_{OC} values for photovoltaic devices comprising blends of the synthesized fullerene derivatives and the polymer P3HT.

2.3. Solubility of the Fullerene Derivatives

The ability to process a given organic material in solution requires a reasonably high solubility of the compound in some solvent. Chlorobenzene is a typical solvent that is used for the deposition of thin film blends of fullerene derivatives and conjugated polymers during the laboratory scale production of polymer solar cells. The composition and morphology of donor-acceptor blends cast from solution depend on the relative solubility of their components as reported for PCBM-MDMO-PPV blends.[3,11] In particular, the use of chlorobenzene, which is a better solvent for PCBM, drastically improved the performance of the devices compared to those that employed toluene as solvent.[3]

In order to investigate this effect for our materials, we systematically measured the solubility of all fullerene derivatives in chlorobenzene. Obtained values are given in Figure 1 (round brackets) and Table 2. The solubility ranges from as low as 4 mg mL^{-1} to the remarkably high value of ~130 mg mL^{-1}. However, there is no clear correlation between the solubility of the investigated fullerene derivatives and their molecular structures as can be seen from the data shown in Figure 1, e.g., compound **7** which bears an ethyl ester unit is less soluble than **6** which carries a methyl ester function; also, the *n*-propyl derivative **8** is more soluble than the isopropyl and *n*-butyl derivatives **9** and **10**, respectively, etc.

Currently there is no comprehensive theory available on the solubility of fullerenes in organic solvents. Nonetheless, there are several reports in the literature, where it was demonstrated that the solubility of fullerene-based compounds depends on the composition, the crystal structure, and the thermodynamic stability of "solvates" that are formed in the system.[31–34] Solvates are Van der Waals adducts of solutes (dissolved compounds) with solvents. In the simplest case, solubility is determined by the equilibrium of the system schematically outlined in Scheme 2, where "S" denotes the solvent molecules.
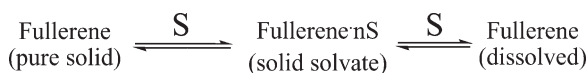
In a first approximation, when a pure solid phase of a fullerene derivative is placed into an organic solvent the fullerene first forms a solvate (adduct) with the solvent. If this solvate is very stable, the energy gain from further solvation is not sufficiently high to break the solvate crystal packing and bring the fullerene molecules into solution. Thus, compounds that form stable crystal adducts with a solvent do not show high solubility in the

Table 1. Reduction potentials of selected fullerene derivatives measured by cyclic voltammetry relative to a standard calomel electrode (SCE) [28].

Compound	$E^1_{1/2}$, [V vs. SCE]	$E^2_{1/2}$, [V vs. SCE]	$E^3_{1/2}$, [V vs. SCE]	$E^4_{1/2}$, [V vs. SCE]
5	−0.76	−1.18	−1.60	−2.12
6	−0.74	−1.12	−1.61	−2.09
7	−0.74	−1.12	−1.61	−2.09
9	−0.74	−1.12	−1.61	−2.09
8	−0.76	−1.16	−1.67	−2.17
10	−0.76	−1.15	−1.68	−2.19
11	−0.76	−1.17	−1.67	−2.29
21	−0.74	−1.14	−1.64	−2.09
23	−0.76	−1.16	−1.67	−2.17
PCBM	−0.76	−1.15	−1.68	−2.19

Table 2. Output parameters of organic solar cells comprising fullerene derivatives **1–27** and P3HT as photoactive materials.

Compound	Solubility [mg · mL^{-1}]	I_{sc}, [mA · cm^{-2}]	V_{oc}, [mV]	FF [%]	η [%]
1	50	10.6	640	55	3.7
2	19	7.9	640	53	2.7
3	36	10.6	600	58	3.7
4	58	7.9	600	33	1.2
5	80	12.2	610	55	4.1
6	10	2.3	407	41	0.4
7	5	0.7	362	36	0.1
8	20*	9.3	550	42	2.2
8	43	8.11	620	43	2.2
9	22	8.4	640	52	2.8
10	30	10.05	620	44	2.7
11	35*	9.6	580	51	2.8
11	106	8.42	620	49	2.5
12	5	0.4	350	35	0.05
13	12	7.3	620	30	1.2
14	10	6.5	560	40	1.7
15	35	11.1	660	49	3.6
16	30	7.8	640	35	1.7
17	23**	8.4	600	50	2.5
18	45	10.16	600	54	3.4
19	70	9	600	53	2.9
20	130	4.6	590	41	1.1
21	124	4.4	590	43	1.1
22	31	10.2	600	45	2.8
23	23	7.61	620	43	2.0
24	25	8	580	45	2.1
25	4	0.2	320	31	0.02
26	11	5.1	580	29	0.9
27	9	2.11	340	37	0.3

same solvent. It is also known that solvates with tight molecular crystal packing demonstrate high thermodynamic stability (i.e., high enthalpies of decomposition).[35] In other words, the solubility of fullerene derivatives correlates with the tightness of their joint packing with solvent molecules within the crystal lattice.

Theoretical simulation of supramolecular fullerene derivative-solvent packing systems is challenging as it is currently not possible to predict a crystal structure formed by two or more co-crystallizing components. Although some theoretical models that explain the solubility of pristine fullerenes in organic solvents have been reported,[36,37] these methods used thereby are hardly applicable to fullerene derivatives. Therefore, the solubility of a new fullerene derivative in a given solvent cannot be predicted with high accuracy but has to be measured experimentally instead.

The common assumption that the solubility of fullerene derivatives can be fully controlled by simply appending larger or smaller, branched or linear ''solubilizing'' groups is not valid for the studied fullerene derivatives. This can be exemplified by a series of compounds bearing methyl (**6**), ethyl (**7**), n-propyl (**8**), isopropyl (**9**), and n-butyl residues (**10**) for which the solubilities in chlorobenzene are as follows: 8, 6, 43, 16, and 30 mg mL^{-1}, respectively.

Another fact that makes the solubility of fullerene derivatives in organic solvents a challenging problem is that it is almost impossible to handle a pure phase of any fullerene-based material. Fullerenes and their derivatives have considerably large cavities in their crystal packing that can be easily filled by solvent or gases molecules (e.g., oxygen, nitrogen, carbon dioxide, toluene, xylene, other solvents).[32] If preparation and purification of a fullerene derivative are carried out in a solvent, the solvent will be trapped within the final product in the form of solvates. For example, any commercially available unsublimed C_{60} contains 3–4% solvent.[38] The same applies to PCBM which is usually provided as solvate with toluene and residual amounts of 1,2-dichlorobenzene or some aliphatic solvent (e.g., hexane.).[39] Therefore, when a fullerene-based material is dissolved we usually start from its solvate with a solvent that was trapped during preparation/purification. This solvent is designated as ''solvent-1'' below. It makes no difference for the outcome if the material is dissolved in a solvent-2 which forms much more stable solvates than solvent-1. However, if more stable solvates are formed between solvent-1 and the fullerene derivative, their solubility might be lower than the solubility of pure fullerene derivative. At the least, dissolution of such solvates in solvent-2 will require more time, limited by cleavage of "fullerene·S1" adducts (Scheme 3).
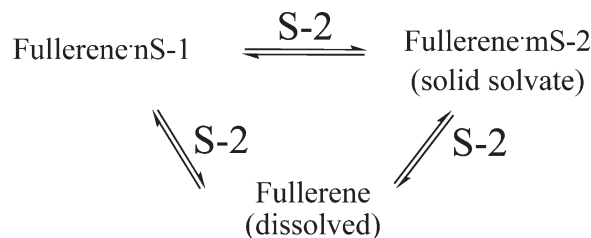
Scheme 3. Equilibrium illustrating the dissolution of a fullerene derivative solvate in a solvent.

Scheme 2. Equilibrium illustrating the dissolution of a pure fullerene derivative in a solvent.

In our experiments this effect was observed for compounds **3**, **18**, and **19**. Depending on the final solvent that was used during the purification procedure different samples of these compounds showed significant variation in their solubility in chlorobenzene. In particular, samples washed with diethyl ether possessed a two times lower solubility than samples of the same compound washed with methanol. NMR spectroscopy showed that these fullerene derivatives form stable 1:1 solvates with diethyl ether, which do not decompose, even at elevated temperatures, while adducts with methanol possess a lower stability and therefore readily decompose within a few days at room temperature. Noteworthy is the fact that the fullerene derivatives themselves showed no signs of oxidation and/or polymerisation or other kind of degradation. Furthermore, different solvates of the same material that exhibit a different solubility also showed differences in performance of the resulting photovoltaic devices.

2.4. Solar Cells Built with the Fullerene Derivatives

All fullerene derivatives shown in Figure 1 were tested in organic solar cells comprising P3HT as donor material. The layout of the devices is outlined schematically in Figure 2a. The typical procedure for the fabrication of solar cells is described in detail in the experimental section. Initially all materials were processed in a very similar way, i.e., the same fullerene:P3HT ratio, spin-coating regime, and annealing temperature/time were used. At least 20 devices were fabricated per material to ensure that reproducibility of results. All materials that yielded power conversion efficiencies of more than 1.0% in these preliminary tests were investigated further and optimized to achieve maximal performance. At this optimization stage the following parameters that are known to influence solar cell performance were varied independently: i) fullerene:polymer ratio from 5:6 to 1:2, ii) spin-coating frequency from 400 to 1 800 min^{-1}, iii) annealing time from 1 to 15 min, and iv) annealing temperature from 150 to 175 °C. As a result, optimal device fabrication procedures were obtained for each fullerene-based material.

Table 2 lists the output parameters obtained for organic solar cells built with fullerene derivatives **1–27** and P3HT at 100 mW cm^{-2} AM 1.5 simulated solar irradiation. The power conversion efficiencies range from 0.02% to 4.1% depending on the nature of the fullerene derivative. Figure 2b exemplifies the *I-V* curves obtained for photovoltaic devices fabricated from the best-performing fullerene derivatives **3**, **5** ([70]PCBM), and **15** as well as those of reference devices fabricated from [60]PCBM. C_{70}-derivatives **5** and **15** gave higher current densities than the very similar C_{60} derivatives **1** and **3**. This is due to the optical properties of C_{70}, which absorbs more light in the visible region than C_{60}.

Figure 2c shows the incident photon-to-current conversion efficiency (IPCE) spectra for photovoltaic devices built with fullerene derivatives **1**, **3**, **5**, and **15**. Comparing the C_{60} derivatives **1** and **3** to their C_{70} relatives **5** and **15** shows that latter ones provide higher IPCE values than the former ranging from 350 to 500 nm. Additionally, there are minor additional features at 660–740 nm apparent within the IPCE spectra of devices comprising C_{70} derivatives. However, the IPCE spectrum of the device fabricated from compound **5** is remarkably red-shifted in comparison to those of all other materials. This strong
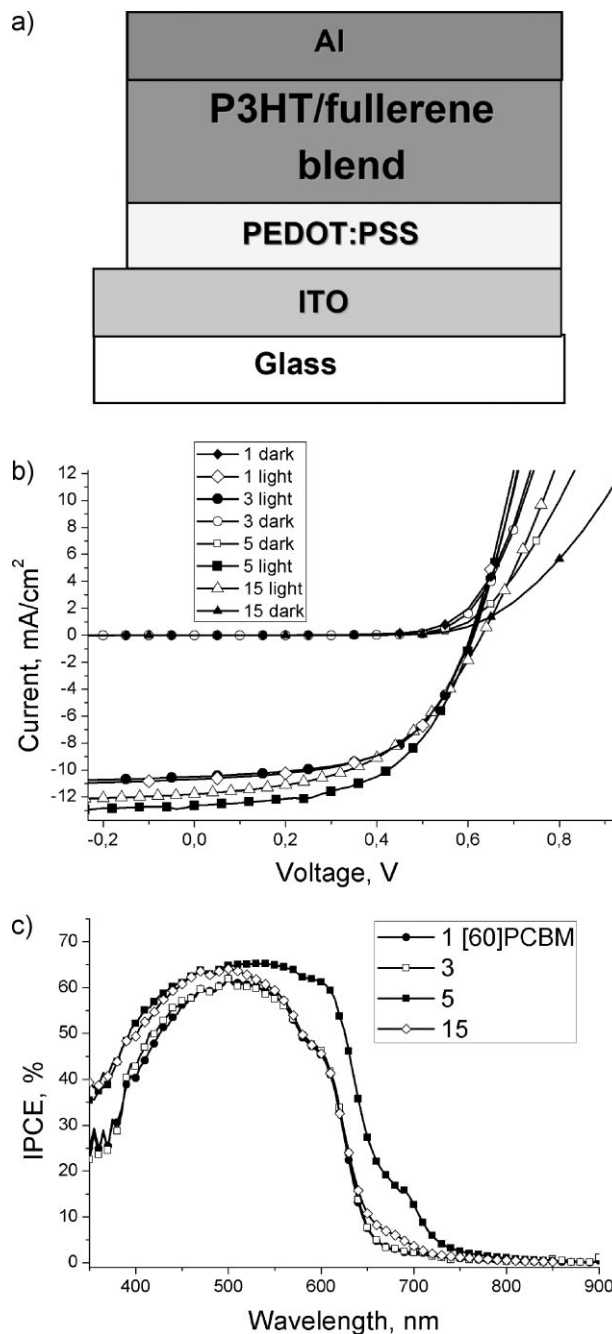

Figure 2. a) Schematic of the solar cell architecture; b and c) representative *I-V* curves and incident photon-to-current conversion efficiency (IPCE) spectra, respectively, for devices comprising different fullerene-based materials.

red-shift of the IPCE spectra was evident for 12 examined devices produced with two independently prepared batches of material **5** and two different batches of P3HT (obtained from Rieke Metals and Plextronics).

Usually, red-shifts in absorption and IPCE spectra of fullerene/P3HT blends are related to an order of the polymer phase and formation of crystalline nanodomains.[40] In the case of compound **5** it seems that there is some (short- or long-range)

polymer phase order that makes this system very promising for an application in organic photovoltaics. The observed effect is currently undergoing further investigation.

2.5. The Solubility–Solar Cell Performance Relationship

Very similar fullerene compounds regularly show considerably different performances in solar cells as can be concluded from the data listed in Table 2 (e.g., compounds **7** and **8** or **13** and **15**). Therefore, a similar structure of the materials does not necessarily result in similar performance. In contrast, even less structurally similar fullerene derivatives give more or less the same output parameters in photovoltaic devices if their solubility values are very close (e.g., compounds **9**, **17**, **23**, and **24**). Therefore, we analyzed the characteristics of organic solar cells as a function of the solubility of the used fullerene derivatives.

Figure 3 illustrates the dependence of the short circuit current (I_{SC}), the open circuit voltage (V_{OC}), the fill factor (FF), and the power conversion efficiency (η) of solar cells on the solubility of the fullerene derivative used as active materials. Note that each point in the plots represents an individual fullerene-derivative. The numbering of the points corresponds to the numbering of the compounds shown in Figure 1. Virtually all compounds were tested using chlorobenzene as a solvent for casting the films. However, some compounds were also tested in devices that were built using toluene (points marked with *) or carbon disulfide (points marked with **) as solvents during active layer deposition.

The I_{SC} (Fig. 3a) rapidly increases with increasing fullerene solubility from 0 to 20 mg mL^{-1}, subsequently approaches a maximum between 30 and 70 mg mL^{-1} and decreases when the

fullerene solubility exceeds 100–110 mg mL^{-1}. Compounds **5** and **15** give the highest current densities in solar cells because they are derived from [70]fullerene and therefore absorb more light than similar derivatives of [60]fullerene. Compound **5** is also different from all other compounds because of the remarkably red-shifted photocurrent response observed for its blends with P3HT (Fig. 2c) which results in higher current densities.

A rapid increase in V_{OC} (Fig. 3b) is observed when the solubility of the fullerene derivative increases from 0 to 20 mg mL^{-1} which resembles the trend observed for I_{SC}. However, a further increase in fullerene solubility does not affect V_{OC} as significantly as I_{SC} but rather keeps it constant at 600 ± 20 mV. The plot for the fill factor (Fig. 3c) shows a clear maximum for fullerene derivatives which exhibit a solubility in the range of ~40–90 mg mL^{-1}. Note that all studied fullerene derivatives have similar LUMO energy levels which should lead to similar V_{OC} values of the photovoltaic devices. Therefore, the actually observed differences in V_{OC} of solar cells with different fullerene derivatives are not related to the energy levels of the compounds but are caused by other effects that are governed by their solubility.

All solar cell parameters were found to be dependent on the solubility of the fullerene derivative used as acceptor material. As a result, the power conversion efficiency of the tested solar cells is also a function of fullerene component solubility, as illustrated in Figure 3d. The maximum of the interpolation curve corresponds to solubility values ranging from 30 to 80 mg · mL^{-1}. However, excluding compound **5** ([70]PCBM) the optimal solubility window is more narrow and ranges from about 30 to 50 mg mL^{-1}. The well known standard fullerene derivative [60]PCBM (solubility of ~50 mg mL^{-1}) exactly fits this window, which explains the high performance of solar cells comprising [60]PCBM and P3HT.

Some compounds, namely **4**, **8** and **16**, do not follow the general trends outlined in the previous section; in particularly the fill factor (Fig. 3c) and hence the overall power conversion efficiency (Fig. 3d) are different. These exceptions will be studied in more detail in the future. Our preliminary results only allow us to suggest some explanations for the observed low performance of compounds **8** and **16**. Compound **8** was found to form unstable solvates with chlorobenzene which decompose when a blend of **8** with P3HT is annealed at 155 °C. The rapid release of the solvent vapor from the film results in a significant disturbance of the film nanostructure ("foaming"). Moreover, the solvent gas bubbles also perforate the aluminum electrodes deposited on top of the film, which is easily seen with the naked eye. Apparently the same occurs with blends of **16** and P3HT during thermal annealing since the aluminum electrodes are also perforated in these cases. As a consequence we note that the solubility of the fullerene derivative allows us to estimate its maximal performance in organic solar cells. However, some side effects can disturb the device structure and thereby lower the performance of the given material.
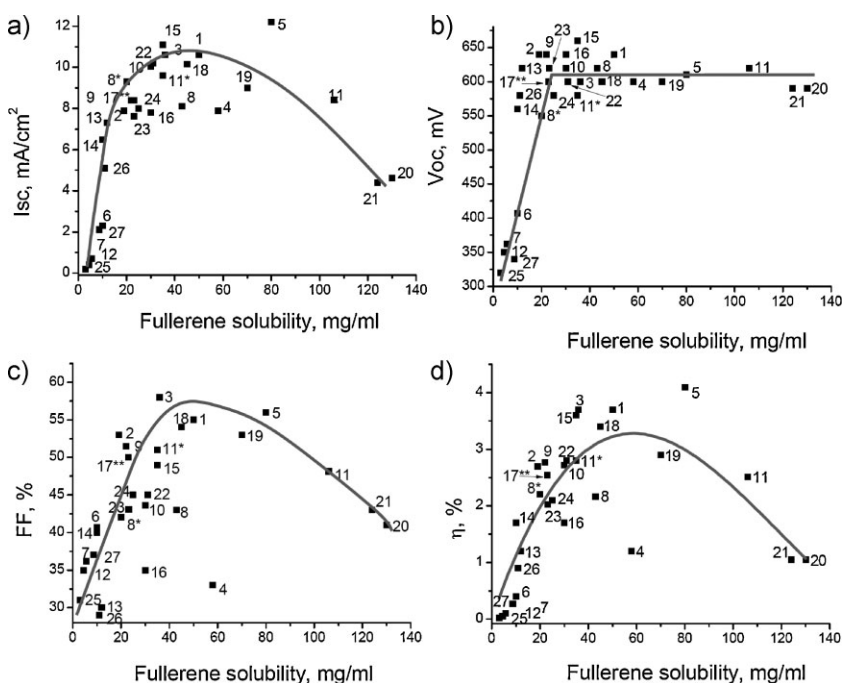

Figure 3. a–d) Relationship between solar cell output parameters (I_{sc}, V_{oc}, FF, and η, respectively) and solubility of the fullerene derivative used as electron acceptor material in the active layer. The lines are included as a guide for the eye.

2.6. The Relationship Between Degree of Phase Separation and Solubility of Fullerene Derivatives

In order to gain an understanding of why and how the solubility of fullerene-based materials affects their solar cell output parameters, we performed optical microscopy and atomic force microscopy (AFM) examinations of the surface topology of films prepared from different fullerene derivatives blended with P3HT. Optical microscopy revealed the presence of very large aggregates 50–100 μm in size in the case of films formed from 7/P3HT blends. We assume that these aggregates represent a pure phase of 7 which crystallizes from the solution during film deposition since 7 is one of the compounds with the lowest solubility in chlorobenzene ($S = 5$ mg · mL^{-1}). The fullerene derivative 6 has a two times higher solubility than 7, hence non-annealed films of 6/P3HT blends exhibit no structural inhomogeneities on their surface which could be detected by optical microscopy or AFM. However, thermal annealing results in the formation of aggregates sized 5–10 μm, but this is still 10 times smaller than the agglomerates observed in 7/P3HT blends. A further increase in solubility of the fullerene-based material to 22 or 30 mg mL^{-1} (compounds 9 or 10, respectively) was found to be sufficient to avoid any large-scale segregation of the components in the P3HT blends even after thermal annealing. At least, no distinct features, which would indicate phase separation on a scale larger than 100–200 nm, were observed on the film surfaces by AFM. Thermal annealing merely results in some roughening of the films surfaces as observed for the blends of P3HT with compounds 9, 10, and PCBM. However, no such roughening was observed for compounds 20 and 21 which possess the highest solubility. Presumably, in this case fullerene derivative and polymer are perfectly intermixed with each other and heating does not induce segregation of the components.

Thus, the microscopy studies performed on the films of fullerene derivatives 6, 7, 9, 10, 20, and [60]PCBM blended with P3HT revealed a general relationship between the solubility of the fullerene derivatives and the topology of their blends with P3HT. AFM and optical data obtained for films comprising other fullerene derivatives were in agreement with the trend observed for compounds 6, 7, 9, and 10 with a few rare exceptions. Amongst them were blends of 4 with P3HT that demonstrated large irregularities on the film surface which suggests a high degree of phase separation in spite of the high solubility of 4 in chlorobenzene.

Generally, if the solubility of a fullerene derivative in chlorobenzene is below 20 mg mL^{-1}, it forms aggregates when blended with P3HT that are directly observable in the films by means of optical microscopy. The appearance of such aggregates reflects that large scale phase separation occurs within the blends. The size of the aggregates is larger for compounds with lower solubility. Therefore, one can assume that these aggregates comprise pure fullerene derivatives that precipitate from the solution whilst the films are prepared. Also, the fullerene aggregates always increase in terms of size during thermal annealing of the blends.

The nanomorphology of fullerene-P3HT blends influences their performance in solar cells.[3] It seems there is a direct correlation between the scale of phase separation in the blends of our compounds with P3HT and the output parameters of solar cells comprising the blends in their active layers. A significant improvement of solar cell performance is observed for the series of compounds comprising 7, 6, and 9 which correlates to an improvement in film morphology, as evident from the microscopy images shown in Figure 4. Moreover, this trend is also observed for compounds 10 and [60]PCBM which have a higher solubility than 9, even though AFM does not show an additional improvement in the active layer surface topology. The relationship between the degree of phase separation, as monitored by optical microscopy and AFM, and the solar cell output parameters was evident for all studied compounds with a solubility below 80 mg · mL^{-1}. There were only a few exceptions, namely compounds 8 and 16, which are discussed above, and compound 3, which will be considered elsewhere. Due to the results that were obtained we conclude that fullerene derivatives should be sufficiently soluble in order to achieve optimal film morphology of their blends with the donor polymer P3HT and hence provide high power conversion efficiencies in solar cells. To avoid the formation of large fullerene aggregates it is necessary to ensure a minimum solubility of 20 mg mL^{-1}. However, a further increase in solubility to 30–40 mg mL^{-1} seems to be beneficial for device performance too.

It is somewhat surprising that fullerene derivatives with a solubility of more than 90–100 mg mL^{-1} in chlorobenzene demonstrate lower performances in solar cells. We believe that such highly soluble fullerene compounds become infinitely intermixable with P3HT, which means that the fullerene-polymer blend is represented as a homogeneous solid solution without phase separation. However, a minimum degree of phase separation is necessary in providing a percolation pathway for charge transport to the electrodes. The optimal degree of phase separation of the components of a bulk heterojunction solar cell was estimated to be in the range of the exciton diffusion length in these materials, which is usually about 5–15 nm.[41]

3. Conclusions

In conclusion, we showed that the solubility of fullerene derivatives influences the nanomorphology of their blends with P3HT. The optimal solubility that results in the highest solar cell performances in combination with P3HT is in the range of 30 to 80 mg mL^{-1} (Fig. 3d). Notably, 50–70 mg mL^{-1} is the maximal solubility of P3HT in chlorobenzene at room temperature. Therefore, the best results were obtained for fullerene derivatives which exhibit a solubility that matches the solubility of the donor polymer P3HT. Consequently, we propose that any novel donor polymers should be tested in organic solar cells with fullerene derivatives that have a similar solubility in the used solvent.

The suggested relationship between the solubility of fullerene derivatives and the donor polymer might help to evaluate new donor polymers in organic solar cells using appropriate fullerene derivatives as acceptor counterparts instead of conventional [60]PCBM. Taking into account the solubility effects described above, correct material combinations, which show advanced performance in organic solar cells, should be obtained by employing donor and acceptor components with similar solubility.
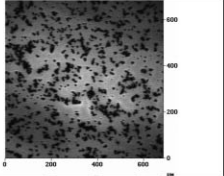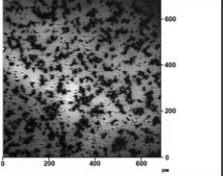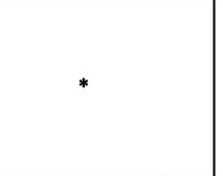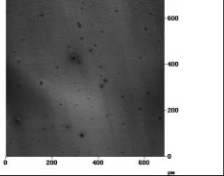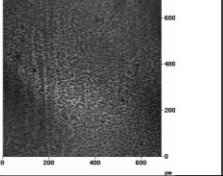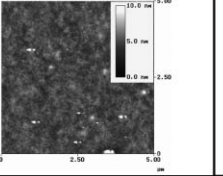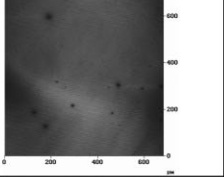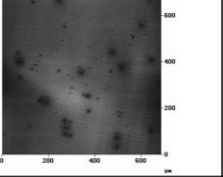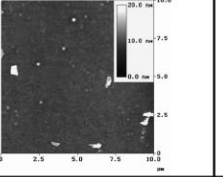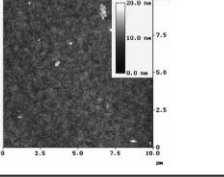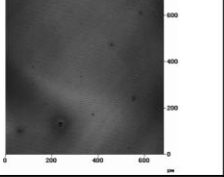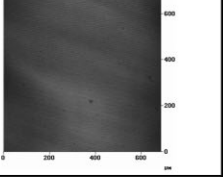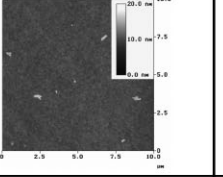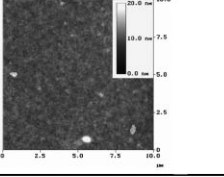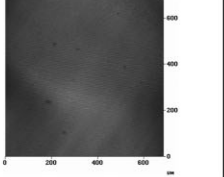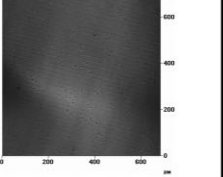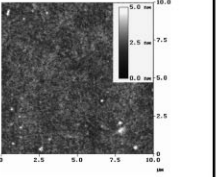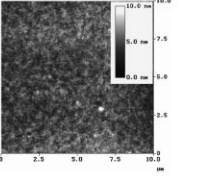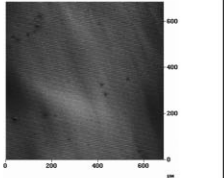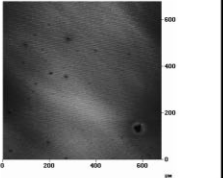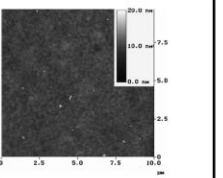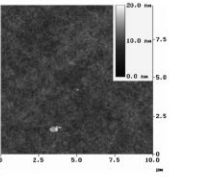
No	S mg/ml	Optical microscopy		AFM	
		Before annealing at 150 C	After annealing at 150 C	Before annealing at 150 C	After annealing at 150 C
7	5			*	*
6	10				*
9	22				
10	30				
1 [60]-PCBM	50				
20	130				

Figure 4. Observed change in blend morphology/surface topology upon increasing the solubility of the fullerene component [*atomic force microscopy (AFM) images are not shown because the scale of phase separation (i.e., size of the aggregates) in these films is larger than the scale of the AFM images (10 μm). In such cases AFM does not provide information about the entire film topology, but rather reflects the surface roughness of either the aggregates themselves or the region between the aggregates in the films depending on the selected area].

4. Experimental

General: All solvents and reagents for syntheses were purchased from Aldrich or Acros Organics and used as received or purified according to standard procedures. Pristine fullerenes C_{60} and C_{70} were purchased from ZAO Fullerene Centre, Russia. Anhydrous solvents provided by Aldrich were used for deposition of fullerene/polymer blends. Two samples of poly(3-hexylthiophene) were used; one was purchased from Rieke Metals Inc. (E-grade), the other was provided by Plextronics.

Synthesis of Fullerene Derivatives: Unless specified otherwise fullerene derivatives were synthesized following a procedure described by Hummelen and Wudl [24]. Compound **26** was prepared via the Bingel-Hirsch route [25,26]. Nucleophilic cyclopropanation with sulfonium ylides, which was first applied to fullerene derivatization by Wilson [27], was used to obtain **27**. Spectroscopic characterization of all compounds was performed using one-dimensional ^{1}H and ^{13}C NMR spectra. Two-dimensional H-H COSY as well as H-C HSQC and HMBC were used to verify the structure assignment for some representative compounds. Detailed synthetic procedures for the preparation of compounds **6–11** and their spectroscopic characterization were published previously [28]. Synthesis and investigation of other compounds will be reported elsewhere.

Cyclic Voltammetry: Cyclic voltammetry measurements were performed using approximately 1×10^{-3} M solutions of the fullerene derivatives in rigorously dried 1,2-dichlorobenzene in a cell equipped with a glassy carbon working electrode (2 mm^2), platinum wires as counter electrodes, and a standard calomel electrode (SCE) as reference electrode. The scan rate was 200 mV s^{-1}. A 0.1 M solution of Bu_4NPF_6 was used as supporting electrolyte.

Solubility measurements: Saturated solutions of fullerene derivatives in chlorobenzene were prepared by stirring of excess solid material in the solvent for at least 10 days. For this purpose, fullerene derivatives were

added in small portions (∼10 mg each) to 1–2 mL of pure solvent. When this first portion of the materials was dissolved, additional 10 mg portions were added to the stirred solutions one after the other until some solid remained undissolved. At this point, further 10 mg were added to ensure the presence of an excess amount of solid material before the mixture was stirred for 7–10 days to achieve equilibrium state in the system. As-prepared saturated solutions were filtered through 0.45-μm PTFE syringe filters into glass containers of known mass. Immediately after filtration the solution was weighted and then left in air to facilitate solvent evaporation. Usually 24 h were sufficiently long to evaporate 1–2 mL of chlorobenzene and reach constant weight for the container with the solid residue. Alternatively, this procedure can be performed in a vacuum desiccator, but some precautions are necessary to avoid rapid solvent evaporation and spilling of materials out of their containers. The volume of the solvent was calculated from the weight loss of the container during solvent evaporation by dividing it by the solvent density. The mass of dissolved material was assumed as being equivalent to the difference between the weight of an empty container and the same container with a solid residue after solvent evaporation. One should note that residues were always present as chlorobenzene solvates of the fullerene derivatives (solid state adduct) with compositions varying between 1:0.5 and 1:2 (fullerene:solvent molecules) as derived from thermogravimetric analysis data. This solvation effect results in an overestimation of the solubility by 4–10%. However, the difference in solubility between any two fullerene derivatives is usually 10–20 times larger than this 4–10% inaccuracy. Therefore, the effect of solvate formation was neglected in our solubility estimations.

Fabrication of solar cells: Fullerene derivatives and P3HT were dissolved together in chlorobenzene to achieve polymer concentrations as high as 12 mg mL^{-1}. The weight ratio between the fullerene derivative and P3HT was varied between 1:2 and 5:6. Resulting fullerene/polymer solutions were filtered through 0.45-μm PTFE syringe filters. ITO glass slides, 15 × 15 mm^2 or 25 × 25 mm^2 in size, were cleaned by consecutive sonication in toluene, acetone and, finally, isopropanol. On top of these clean ITO surfaces a layer of PEDOT-PSS solution (Baytron PH) was spin-coated at 3 000 min^{-1}. The PEDOT-PSS films were then annealed at 175 °C for 15 min before the fullerene-polymer blends were spin-coated on top. Initially, fullerene derivative/P3HT blends were deposited at a spin-coating frequency of 900 min^{-1} which is the optimum frequency for PCBM/P3HT deposition. In subsequent (optimization) experiments the spin-coating frequency was varied within a range of 400–1500 min^{-1} in order to establish the best active layer deposition conditions for every studied system. Usually, such optimization resulted in an approximately 1–10% increase of the solar cell power conversion efficiency, which is a relatively modest improvement when compared to the fullerene solubility effects studied in this work.

Solar cell output parameters were virtually identical for devices regardless of whether the active layer was deposited inside or outside a nitrogen glove-box. Fullerene-polymer blend films were dried under vacuum (∼10^{-3} mbar) at ambient temperature for 1–2 h, before 100–200 nm thick aluminum top electrodes were deposited in high vacuum ∼10^{-6} mbar. Finalized devices were annealed at temperatures in the range of 150–170 °C for 2–15 min. For each binary system the optimal conditions, i.e., fullerene derivative:P3HT component ratio, spin-coating frequency, and annealing temperature/time, were determined experimentally. Generally, the most reproducible and reliable procedure involved a 2:3 fullerene:P3HT ratio, 800 min^{-1} spinning frequency, and device annealing at 160 °C for 5 min. *I–V* characteristics of the devices were obtained in the dark and under simulated 100 mW cm^{-2} AM1.5 solar irradiation that latter of which was provided by a KHS Steuernagel solar simulator. The intensity of the illumination was verified prior to each individual measurement using a calibrated silicon diode with known spectral response. Data reported is not corrected for the mismatch between solar simulator illumination and AM1.5 spectrum. Performances of the best performing cells were cross-checked using different solar simulators in at least two independent laboratories (LIOS, Linz, Austria; TITK, Rudolstadt, Germany; IPCP RAS, Chernogolovka, Russia), which gave very similar results. Photocurrent spectra were measured on a SRS 830 lock-in amplifier using the monochromated light from a 75 W Xe lamp as excitation source.

[1] H. Hoppe, N. S. Sariciftci, *J. Mater. Res.* **2004**, *19*, 1924.

[2] K. M. Coakley, M. D. McGehee, *Chem. Mater.* **2004**, *16*, 4533.

[3] H. Hoppe, N. S. Sariciftci, *J. Mater. Chem.* **2006**, *16*, 45.

[4] H. Hoppe, N. S. Sariciftci, in *Photoresponsive Polymers II*, Series: Advances in Polymer Science, Vol. *214* (Eds: S.R. Marder, K.- S. Lee), Springer, Berlin, Germany **2008**, pp. 1–86.

[5] B. C. Thompson, J. M. J. Frechet, *Angew. Chem, Int. Ed.* **2008**, *47*, 58.

[6] N. S. Sariciftci, D. Braun, C. Zhang, V. I. Srdanov, A. J. Heeger, G. Stucky, F. Wudl, *Appl. Phys. Lett.* **1993**, *62*, 585.

[7] J. Peet, J. Y. Kim, N. E. Coates, W. L. Ma, D. Moses, A. J. Heeger, G. C. Bazan, *Nat. Mater.* **2007**, *6*, 498.

[8] J. Y. Kim, K. Lee, N. E. Coates, D. Moses, T.-Q. Nguyen, M. Dante, A. J. Heeger, *Science* **2007**, *317*, 222.

[9] S.-S. Kim, S.-I. Na, J. Jo, G. Tae, D.-Y. Kim, *Adv. Mater.* **2007**, *19*, 4410.

[10] G. Yu, J. Gao, J. C. Hummelen, F. Wudl, A. J. Heeger, *Science* **1995**, *270*, 1789.

[11] S. E. Shaheen, C. J. Brabec, N. S. Sariciftci, F. Padinger, T. Fromherz, J. C. Hummelen, *Appl. Phys. Lett.* **2001**, *78*, 841.

[12] A. Mozer, P. Denk, M. Scharber, H. Neugebauer, N. S. Sariciftci, P. Wagner, L. Lutsen, D. Vanderzande, *J. Phys. Chem. B* **2004**, *108*, 5235.

[13] M. M. Wienk, J. M. Kroon, W. J. H. Verhees, J. Knol, J. C. Hummelen, P. A. van Hall, R. A. J. Janssen, *Angew. Chem, Int. Ed.* **2003**, *42*, 3371.

[14] F. Padinger, R. S. Rittberger, N. S. Sariciftci, *Adv. Funct. Mater.* **2003**, *13*, 85.

[15] P. Schilinsky, C. Waldauf, C. Brabec, *Adv. Funct. Mater.* **2006**, *16*, 1669.

[16] H. Hoppe, S. Shokhovets, G. Gobsch, *Phys. Status Solidi RRL* **2007**, *1*, R40.

[17] V. Shrotriya, G. Li, Y. Yao, T. Moriarty, K. Emery, Y. Yang, *Adv. Funct. Mater.* **2006**, *16*, 2016.

[18] A. J. Moule, K. Meerholz, *Adv. Mater.* **2008**, *20*, 240.

[19] W. Ma, C. Yang, X. Gong, K. Lee, A. J. Heeger, *Adv. Funct. Mater.* **2005**, *15*, 1617.

[20] M. Svensson, F. Zhang, S. C. Veenstra, W. J. H. Verhees, J. C. Hummelen, J. M. Kroon, O. Inganas, M. R. Andersson, *Adv. Mater.* **2003**, *15*, 988.

[21] F. Zhang, K. G. Jespersen, C. Björström, M. Svensson, M. R. Andersson, V. Sundström, K. Magnusson, E. Moons, A. Yartsev, O. Inganäs, *Adv. Funct. Mater.* **2006**, *16*, 667.

[22] L. H. Slooff, S. C. Veenstra, J. M. Kroon, D. J. D. Moet, J. Sweelssen, M. M. Koetse, *Appl. Phys. Lett.* **2007**, *90*, 143506.

[23] D. Muhlbacher, M. Scharber, M. Morana, Z. Zhu, D. Waller, R. Gaudiana, C. Brabec, *Adv. Mater.* **2006**, *18*, 2884.

[24] J. C. Hummelen, B. W. Knight, F. Lepeq, F. Wudl, J. Yao, C. L. Wilkins, *J. Org. Chem.* **1995**, *60*, 532.

[25] C. Bingel, *Chem. Ber.* **1993**, *126*, 1957.

[26] X. Camps, A. Hirsch, *J. Chem. Soc, Perkin Trans. 1* **1997**, 1595.

[27] Y. Wang, J. Cao, D. Schuster, S. R. Wilson, *Tetrahedron Lett.* **1995**, *36*, 6843.

[28] J. Y. Mayorova, S. L. Nikitenko, P. A. Troshin, S. M. Peregudova, A. S. Peregudov, M. G. Kaplunov, R. N. Lyubovskaya, *Mendeleev Commun.* **2007**, *17*, 175.

[29] C. J. Brabec, A. Cravino, D. Meissner, N. S. Sariciftci, T. Fromherz, M. T. Rispens, L. Sanchez, J. C. Hummelen, *Adv. Funct. Mater.* **2001**, *11*, 374.

[30] F. B. Kooistra, J. Knol, F. Kastenberg, L. M. Popescu, W. J. H. Verhees, J. M. Kroon, J. C. Hummelen, *Org. Lett.* **2007**, *9*, 551.

[31] R. S. Ruoff, R. Malhortra, D. L. Huestis, D. S. Tse, D. C. Lorents, *Nature* **1993**, *362*, 140.

[32] Y. Marcus, A. L. Smith, M. V. Korobov, A. L. Mirakyan, N. V. Avramenko, E. B. Stukalin, *J. Phys. Chem. B* **2001**, *105*, 2499.

[33] M. V. Korobov, A. L. Mirakian, N. V. Avramenko, E. F. Valeev, I. S. Neretin, Y. L. Slovokhotov, A. L. Smith, G. Olofsson, R. S. Ruoff, *J. Phys. Chem. B* **1998**, *102*, 3712.

[34] P. A. Troshin, Yu, A. Mackeyev, N. V. Chelovskaya, Yu, L. Slovokhotov, O. V. Boltalina, L. N. Sidorov, *Fullerene Sci. Techn.* **2000**, *8*, 501.

[35] Y. A. Makeev, P. A. Troshin, O. V. Boltalina, M. A. Kirikova, N. V. Chelovskaya, *Phys. Solid State* **2002**, *44*, 536.

[36] E. B. Stukalin, M. V. Korobov, N. V. Avramenko, *J. Phys. Chem. B* **2003**, *107*, 9692.

[37] A. A. Toropov, B. F. Rasulev, D. Leszczynska, J. Leszczynski, *Chem. Phys. Lett.* **2007**, *444*, 209.

[38] Yu. M. Shulga, V. M. Martynenko, S. A. Baskakov, Yu. V. Baskakova, G. A. Volkov, N. V. Chapysheva, V. F. Razumov, V. G. Sursaeva, *Mass-spektrometriya* **2005**, *2*, 223 (in Russian).

[39] P. A. Troshin, unpublished. (^{1}H NMR analysis of PCBM samples that were provided by Nano-C Corp, Solenne BV, American dye source Inc, MTR LTD, and SES research).

[40] T. Erb, U. Zhokhavets, G. Gobsch, S. Raleva, B. Stuhn, P. Schilinsky, C. Waldauf, C. Brabec, *Adv. Funct. Mater.* **2005**, *15*, 1193.

[41] P. W. M. Blom, V. D. Mihailetchi, J. A. Koster, D. E. Markov, *Adv. Mater.* **2007**, *19*, 1551.